Attractor Sets and Quasi-Geostrophic Equilibrium

EDWARD N. LORENZ

Department of Meteorology, Massachusetts Institute of Technology, Cambridge 02139

(Manuscript received 9 January 1980, in final form 8 April 1980)

ABSTRACT

The attractor set of a forced dissipative dynamical system is for practical purposes the set of points in phase space which continue to be encountered by an arbitrary orbit after an arbitrary long time. For a reasonably realistic atmospheric model the attractor should be a bounded set, and most of its points should represent states of approximate geostrophic equilibrium.

A low-order primitive-equation (PE) model consisting of nine ordinary differential equations is derived from the shallow-water equations with bottom topography. A low-order quasi-geostrophic (QG) model with three equations is derived from the PE model by dropping the time derivatives in the divergence equations.

For the chosen parameter values, gravity waves which are initially present in the PE model nearly disappear after a few weeks, while the quasi-geostrophic oscillations continue undiminished. The states which are free of gravity waves form a three-dimensional stable invariant manifold within the nine-dimensional phase space. Points on this manifold are readily found by an algorithm based on the separation of time scales. The attractor set consists of a complex of two-dimensional surfaces embedded in this manifold. The geostrophic equation is a good approximation on most of the attractor, while the balance equation is better. The attractors of the PE and QG models are qualitatively similar.

Some speculations regarding the invariant manifold and the attractor in a large global circulation model are offered.

1. Introduction

The physical laws which govern the behavior of a fluid system are commonly expressed as a set of partial differential equations (PDE's). It is often assumed that we may replace these equations by a large set of ordinary differential equations (ODE's), with time as the independent variable, without seriously altering the properties which interest us most. Such a substitution may in fact be a necessary step in preparing the PDE's for numerical integration. For various reasons, however, we sometimes choose to replace the PDE's by a *small* set of ODE's, hoping that some of the gross qualitative properties of the solutions will not be lost.

In mathematical terminology a set of N ODE's in N dependent variables constitutes a *dynamical system*. It is convenient to treat the N variables as coordinates in an N-dimensional *phase space*. A particular state of the system then becomes a point in phase space, while a particular time-dependent solution becomes an orbit. Periodic solutions become closed orbits, while steady solutions become fixed points.

A point Q is called a *limit point* of a point P, or of the orbit C passing through P, if there exists a set of times $t_1, t_2, \ldots$, approaching infinity, such that the points $P_1, P_2, \ldots$, through which C passes at times $t_1, t_2, \ldots$, approach Q as a limit. It is evident that each point on the orbit passing through Q is then a limit point of each point on C.

A fundamental property of a dynamical system is its *attractor set* A. A point Q is in A if the points for which Q is a limit point together form a set of nonzero volume in phase space. It is evident that each point on the orbit through Q is then in A, so that the attractor is composed of orbits.

A stable (not neutral) fixed point Q must be in A, since Q is a limit point for all points enclosed by some sphere S which encloses Q. None of the remaining points enclosed by S is in A. Likewise, a stable closed orbit C must be part of A, since it is a limit point for all points enclosed by some tube enclosing C. No other points enclosed by this tube are in A. Unstable fixed points and closed orbits need not be in A; in some dynamical systems, however, they are.

For a system where some quantity such as total energy remains invariant, the attractor set, as we have defined it, may be empty. Here the points for which a point Q is a limit point are confined to the energy surface containing Q, which in general possesses zero volume. For a large class of forced dissipative systems, however, which possess no invariants, A is non-void and is itself a set of zero volume.

0022-4928/80/081685-15$07.75

In the present study we shall confine our attention to forced dissipative systems. For well-behaved systems we can be reasonably sure that if we choose a point P at random, the orbit passing through P at some initial time will, at any sufficiently later time, be passing through a point extremely close to A. This makes it possible to estimate the location of A by integrating the ODE's numerically.

If a system is a reasonably realistic model of the earth's atmosphere, we can anticipate some of the properties of its attractor from our experience with weather maps. Thus, we would expect most of the dependent variables to be bounded; we do not, for example, encounter sealevel maps with 1200 mb high-pressure centers or 800 mb lows. Likewise, there are combinations of variables which seldom if ever occur; we do not find maps where the wind blows the wrong way about the principal highs and lows in middle and higher latitudes. Points in the attractor, then, should not be too far removed from the origin, and should correspond to states where the bulk of the atmosphere is in approximate geostrophic equilibrium.

The primary purpose of this study is to find out what the attractor set looks like for some simple atmospheric model. Since we shall be interested in whether or not the points on the attractor tend to represent states of geostrophic equilibrium, we must avoid using a quasi-geostrophic (QG) model, for which no other states exist. We shall therefore choose a primitive-equation (PE) model.

We shall make two comparisons. We shall first compare the attractor with the set of all states where the wind and pressure fields are in exact geostrophic balance. We do not expect these sets to be identical, since in PE models the geostrophic relation is only approximately satisfied. Moreover, in a dry PE model with $3M$ ODE's, derived from a system of three PDE's, the set of all geostrophic states forms an M-dimensional subspace of phase space. The attractor, on the other hand, may be zero- or one-dimensional, if all orbits approach a fixed point or a closed orbit. We shall therefore seek a model where the general solution is aperiodic. A necessary condition for this to be so is that the points on closed orbits (including fixed points) together form a set of zero volume, and that all of these orbits be unstable. Even in this case the attractor need not be M-dimensional; it might have as many as $3M$-1 dimensions.

We shall also compare the attractor with the attractor of a QG model, which we shall derive from the PE model by discarding certain terms, including the time derivative of the divergence. The QG model will have M variables. We shall find that, in some cases at least, the attractor sets of both models will be (M-1) dimensional, and will bear considerable resemblance to one another.

A precise knowledge of the attractor would be of great practical value in numerical weather forecasting. A solution of a PE model originating from an arbitrary initial state generally undergoes rapid large-amplitude gravity-wave oscillations not characteristic of the real atmosphere. This happens even when the initial state has been determined from actual observations, in view of their inevitable omissions and inaccuracies. It should not happen if the initial state lies exactly on the attractor. The familiar initialization problem may therefore be looked upon as the problem of projecting onto the attractor in phase space.

In all dynamical systems where the general solution is aperiodic and the attractor has been determined, it has proven to be a *strange attractor*. That is, it is not topologically the product of several one-dimensional continua, in the sense that a smooth surface in three-dimensional space is the product of two continua. Instead it is the product of several continua and one or more Cantor sets, and an arbitrary intersecting curve, such as a line parallel to a coordinate axis, intersects it in a Cantor set. This is an uncountable nowhere-dense set; an example is the set of all numbers between 0 and 1 whose *decimal* expansions contain only 0's and 1's. For $N = 3$ a strange attractor would be an infinite complex of surfaces.

It is thus evident that except in very simple models a sufficiently precise description of the attractor to allow one to project onto it may be next to impossible. We shall therefore not attempt to study a particularly realistic atmospheric model, and seek instead the simplest model which retains pressure and the two wind components as separate variables and includes the nonlinear interactions which give rise to aperiodicity. For the latter purpose we should represent each variable by at least three functions of time alone. We thus anticipate a system of nine ODE's, and our problem will be to describe the attractor in nine-dimensional phase space.

2. Constraints on the attractor

We shall consider only dynamical systems whose N equations may, after a linear transformation of the dependent variables, if necessary, be written

$$\frac{dw_i}{dt} = \sum_{j,k} a_{ijk} w_j w_k - \sum_j b_{ij} w_j + c_i, \tag{1}$$

where

$$B = \sum_{i,j} b_{ij} w_i w_j > 0, \tag{2}$$

whenever

$$R^2 = \sum_i w_i^2 \tag{3}$$

is positive. Here all summations run from 1 to N.

Many models of forced dissipative fluid systems possess equations of this form. Let A_1, B_1 and C_1 denote, respectively, the maximum of

$$A = \sum_{i,j,k} a_{ijk} w_i w_j w_k, \tag{4}$$

the minimum of B, and the maximum of

$$C = \sum_i c_i w_i \tag{5}$$

on the sphere $R = 1$. Because A and C are of odd degree, $A_1 \geq 0$ and $C_1 \geq 0$, while, because of (2), $B_1 > 0$. It follows that

$$dR/dt \leq A_1 R^2 - B_1 R + C_1. \tag{6}$$

We shall consider only those systems for which

$$B_1^2 - 4A_1 C_1 > 0. \tag{7}$$

If the value of R^2 is conserved by the quadratic terms in (1), $A = 0$, whence $A_1 = 0$, and (7) is automatically satisfied. In this case $dR/dt < 0$ when R exceeds some value R_1. It follows that all orbits ultimately enter and remain within the interior of the sphere $R = R_1 + \epsilon$, where ϵ can be any small positive quantity, whence the attractor must be enclosed by this sphere.

If instead $A_1 > 0$, $dR/dt < 0$ when R lies between two distinct values R_1 and R_2, in view of (7). In this case some orbits may remain outside the outer sphere $R = R_2$ and even go off to infinity, but those orbits passing inside the outer sphere ultimately enter and remain within the interior of a sphere $R = R_1 + \epsilon$. A *component* of the attractor is therefore enclosed by this sphere. The remaining points, if any, of the attractor lie on or outside the sphere $R = R_2$. For such systems we shall consider only the portion of phase space where $R < R_2$.

We shall further restrict our attention to systems where

$$a_{ijk} = 0 \quad \text{if} \quad j = i \quad \text{or} \quad k = i; \tag{8}$$

such systems also include many fluid models. If S is some closed surface, and if the points of S move according to (1), the volume V enclosed by S obeys the equation

$$dV/dt = -V \sum_i b_{ii}. \tag{9}$$

The right side of (9) is negative since B is positive definite. Hence $V \to 0$ exponentially. In particular, by letting S be the sphere $R = R_1 + \epsilon$, we see that at times $\Delta t, 2\Delta t, \ldots$, where $\Delta t > 0$, the attractor, or its bounded component, is enclosed by a succession of surfaces $S_1, S_2, \ldots$, each interior to the previous one, and each enclosing an exponentially smaller volume. Hence the attractor is a set of zero volume.

3. The model

For our physical system we shall choose a homogeneous incompressible fluid of average depth H, moving over a surface of variable topographic height $h(\mathbf{r})$ and unbounded horizontal extent. The fluid moves with horizontal velocity $\mathbf{V}(t,\mathbf{r})$ which is independent of elevation, and a vertical velocity determined by mass continuity, and its upper surface is at elevation $H + z(t,\mathbf{r})$. Here t is time and $\mathbf{r}$ is a horizontal position vector, and the horizontal averages of h and z are zero. We let the system rotate with constant Coriolis parameter f. We allow $\mathbf{V}$ and z to be damped diffusively by small-scale motions, with diffusion coefficients ν and κ, and we let the system be forced by a mass source and sink $F(\mathbf{r})$ which does not vary with time. We must assume, however, that the fluid which is being added at any point possesses the same horizontal velocity as the fluid already at that point. Assuming essentially hydrostatic conditions, we may write the governing equations as

$$\partial \mathbf{V}/\partial t = -(\mathbf{V}\cdot\nabla)\mathbf{V} - f\mathbf{k} \times \mathbf{V} - g\nabla z + \nu\nabla^2\mathbf{V}, \tag{10}$$

$$\partial z/\partial t = -(\mathbf{V}\cdot\nabla)(z - h) - (H + z - h)\nabla\cdot\mathbf{V} + \kappa\nabla^2 z + F, \tag{11}$$

where g is the acceleration of gravity and $\mathbf{k}$ is a unit vertical vector.

Eqs. (10) and (11) are a modified form of the shallow-water equations, which apply when the wave length, but not the wave height, greatly exceeds the depth of the fluid. Our purpose for introducing them, however, is to simulate certain features of atmospheric behavior. Thus, although real water waves are likely to be mechanically driven, the mass source and sink more closely model the thermal forcing of the atmosphere. Likewise, the dissipative term in (11) simulates thermal dissipation. We have not included the familiar "beta" term which would result from a variable f; we note, however, that its effect has been approximated in both theoretical and laboratory models (e.g., von Arx, 1952) by choosing suitable bottom topography.

We now let

$$\mathbf{V} = \nabla\chi + \mathbf{k} \times \nabla\psi, \tag{12}$$

where χ is a velocity potential for the divergent part of $\mathbf{V}$ and ψ is a streamfunction for the rotational part of $\mathbf{V}$, so that $\nabla^2\chi$ and $\nabla^2\psi$ are the divergence and vorticity. Then, after some manipulation, (10) yields the divergence and vorticity equations

$$\partial\nabla^2\chi/\partial t = -\tfrac{1}{2}\nabla^2(\nabla\chi\cdot\nabla\chi) - \nabla\chi\cdot\nabla(\nabla^2\psi) \times \mathbf{k} + \nabla^2(\nabla\chi\cdot\nabla\psi \times \mathbf{k}) + \nabla\cdot(\nabla^2\psi\nabla\psi) - \tfrac{1}{2}\nabla^2(\nabla\psi\cdot\nabla\psi) + \nu\nabla^4\chi + f\nabla^2\psi - g\nabla^2 z, \tag{13}$$

$$\partial\nabla^2\psi/\partial t = -\nabla\cdot(\nabla^2\psi\nabla\chi) - \nabla\psi\cdot\nabla(\nabla^2\psi)\times\mathbf{k} - f\nabla^2\chi + \nu\nabla^4\psi, \quad (14)$$

while (11) becomes

$$\partial z/\partial t = -\nabla\cdot(z-h)\nabla\chi - \nabla\psi\cdot\nabla(z-h)\times\mathbf{k} - H\nabla^2\chi + \kappa\nabla^2 z + F. \quad (15)$$

We shall use (13)–(15) as our basic equations.

To convert (13)–(15) to a low-order model we introduce three dimensionless horizontal vectors $\boldsymbol{\alpha}_1$, $\boldsymbol{\alpha}_2$, $\boldsymbol{\alpha}_3$ for which

$$\boldsymbol{\alpha}_1 + \boldsymbol{\alpha}_2 + \boldsymbol{\alpha}_3 = 0, \quad (16)$$

and, for $(i,j,k) = (1,2,3)$, $(2,3,1)$ or $(3,1,2)$, we let

$$a_i = \boldsymbol{\alpha}_i\cdot\boldsymbol{\alpha}_i, \quad (17)$$

$$b_i = \boldsymbol{\alpha}_j\cdot\boldsymbol{\alpha}_k, \quad (18)$$

$$c_i = \boldsymbol{\alpha}_j\times\boldsymbol{\alpha}_k\cdot\mathbf{k}, \quad (19)$$

and note that

$$b_i = \tfrac{1}{2}(a_i - a_j - a_k), \quad (20)$$

$$c_i = (b_1b_2 + b_2b_3 + b_3b_1)^{1/2} = c. \quad (21)$$

We then choose a length L, and introduce three orthogonal functions

$$\phi_i = \cos(\boldsymbol{\alpha}_i\cdot\mathbf{r}/L), \quad (22)$$

and observe that

$$L^2\nabla^2\phi_i = -a_i\phi_i, \quad (23)$$

$$L^2\nabla\phi_j\cdot\nabla\phi_k = -\tfrac{1}{2}b_i\phi_i + \cdots, \quad (24)$$

$$L^2\nabla\cdot(\phi_j\nabla\phi_k) = \tfrac{1}{2}b_j\phi_i + \cdots, \quad (25)$$

$$L^2\nabla\phi_j\cdot\nabla\phi_k\times\mathbf{k} = -\tfrac{1}{2}c\phi_i + \cdots, \quad (26)$$

where the omitted terms are multiples of cosines of arguments other than those included in (22).

We now let

$$t = f^{-1}\tau, \quad (27)$$

$$\chi = 2L^2f\sum x_i\phi_i, \quad (28)$$

$$\psi = 2L^2f\sum y_i\phi_i, \quad (29)$$

$$z = 2L^2f^2g^{-1}\sum z_i\phi_i, \quad (30)$$

$$h = 2L^2f^2g^{-1}\sum h_i\phi_i, \quad (31)$$

$$F = 2L^2f^3g^{-1}\sum F_i\phi_i, \quad (32)$$

where all summations run from 1 to 3. Substituting (27)–(32) into (13)–(15) and dropping the terms which are omitted in (24)–(26), we obtain the equations of our low-order PE model

$$a_i dx_i/d\tau = a_ib_ix_jx_k - c(a_i - a_k)x_jy_k + c(a_i - a_j)y_jx_k - 2c^2y_jy_k - \nu_0a_i^2x_i + a_iy_i - a_iz_i, \quad (33)$$

$$a_i dy_i/d\tau = -a_kb_kx_jy_k - a_jb_jy_jx_k + c(a_k - a_j)y_jy_k - a_ix_i - \nu_0a_i^2y_i, \quad (34)$$

$$dz_i/d\tau = -b_kx_j(z_k - h_k) - b_j(z_j - h_j)x_k + cy_j(z_k - h_k) - c(z_j - h_j)y_k + g_0a_ix_i - \kappa_0a_iz_i + F_i, \quad (35)$$

where $\nu_0 = L^{-2}f^{-1}\nu$, $\kappa_0 = L^{-2}f^{-1}\kappa$, and $g_0 = HL^{-2}f^{-2}g$. Each of Eqs. (33)–(35) is defined for each cyclic permutation (i,j,k) of (1,2,3).

Without loss of generality we may assume that the vector $\boldsymbol{\alpha}_1$ points northward. The variables with a subscript 1 then represent zonally uniform velocity and height fields, while those with a subscript 2 or 3 represent superposed large-scale waves or eddies.

If we introduce the auxiliary variables

$$U_i = -b_jx_i + cy_i, \quad (36)$$

$$V_i = -b_kx_i - cy_i, \quad (37)$$

and use the components

$$X_i = -a_ix_i \quad (38)$$

of the divergence and

$$Y_i = -a_iy_i \quad (39)$$

of the vorticity as variables in place of x_i and y_i, we may, making liberal use of (20), write (33)–(35) in the more concise form

$$dX_i/d\tau = U_jU_k + V_jV_k - \nu_0a_iX_i + Y_i + a_iz_i, \quad (40)$$

$$dY_i/d\tau = U_jY_k + Y_jV_k - X_i - \nu_0a_iY_i, \quad (41)$$

$$dz_i/d\tau = U_j(z_k - h_k) + (z_j - h_j)V_k - g_0X_i - \kappa_0a_iz_i + F_i. \quad (42)$$

Eqs. (40)–(42) are used in our numerical-integration program.

To construct a simple QG model, we may discard all nonlinear terms and all terms containing the x's, including the time derivative, from (33), and all nonlinear or topographic terms containing the x's from (34) and (35). We then eliminate the x's and z's, and obtain

$$(a_ig_0 + 1)dy_i/d\tau = g_0c(a_k - a_j)y_jy_k - a_i(a_ig_0\nu_0 + \kappa_0)y_i - ch_ky_j + ch_jy_k + F_i, \quad (43)$$

which is again defined for all cyclic permutations (i,j,k) of (1,2,3).

Eq. (43) is fairly general. Without topography it is equivalent to the system used by Vickroy and Dutton (1979) to study bifurcations and catastrophes. With both waves of equal length, with zonally uniform forcing, and with topography in the form of

one wave, it reduces to the system used by Charney and Devore (1979) to study multiple equilibria. Without topography, forcing, or damping it becomes the "minimum equations" used by the author (Lorenz, 1960) to study triad interactions.

If the variables w_i in (1) are identified with the quantities $(a_i g_0 + 1)^{1/2} y_i$ in the QG model (43), B becomes positive definite, while R^2, which may be identified with twice the total energy, is conserved by the quadratic terms. The QG attractor is therefore a bounded set with zero volume. If instead the variables in (1) are identified with suitable linear functions of the variables in the PE model (33)–(35), B again becomes positive definite. However, because the expression for total energy in the shallow-water equations (13)–(15) is not quadratic, it is not positive definite in the truncated equations (33)–(35) derived from (13)–(15), and in fact the quadratic terms in (33)–(35) do not conserve any positive definite quantity, so $A_1 > 0$. It is therefore conceivable that almost all orbits will go to infinity if the forcing is strong, but, when $F_1^2 + F_2^2 + F_3^2$ is sufficiently small, the inequality (7) will be satisfied, and a component of the PE attractor will be bounded, with zero volume. It is this component which we shall investigate, and compare with the QG attractor.

4. Choice of numerical values

As previously noted, we wish to choose the numerical values of the various parameters in the PE model (33)–(35) so that the general solution will be aperiodic. It seems reasonable to expect that we might accomplish this by choosing the parameters to make the general solution of the QG model (43) aperiodic. It is beyond the scope of this study to explore a major portion of parameter space for even so simple a system as (43). We shall therefore turn immediately to a set of values which makes (43) equivalent to a system already known to have an aperiodic general solution. This system is one studied by the author (Lorenz, 1963) in a paper which we shall subsequently refer to as D.

We shall first let $h_2 = h_3 = 0$ and $F_2 = F_3 = 0$, so that the topography and the forcing are zonally uniform. We shall let $a_1 = 1$, so that $2\pi L$ becomes the distance between adjacent latitudes of maximum eastward velocity. We shall choose $a_2 = 1$, and set $a_3 = a$, whence $c^2 = a - a^2/4$. Finally, we shall let $\kappa_0 = \nu_0$.

If we now set

$$y_1' = A'B'h_1[y_1 - \nu_0^{-1}(g_0 + 1)^{-1}F_1], \quad (44)$$

$$y_2' = A'B'h_1 y_2, \quad (45)$$

$$y_3' = A'y_3, \quad (46)$$

$$\tau' = \nu_0 \tau, \quad (47)$$

where

$$A' = \nu_0^{-1}(g_0 + 1)^{-1}g_0 c(a - 1), \quad (48)$$

$$B' = \nu_0^{-1}(ag_0 + 1)^{-1}ca^{-1}, \quad (49)$$

we find that (43) becomes

$$dy_1'/d\tau' = y_2'y_3' - y_1', \quad (50)$$

$$dy_2'/d\tau' = -y_1'y_3' - y_2' + ry_3', \quad (51)$$

$$dy_3'/d\tau' = ay_2' - ay_3', \quad (52)$$

where

$$r = -A'B'[g_0^{-1}(a - 1)^{-1}h_1^2 + \nu_0^{-1}(g_0 + 1)^{-1}h_1F_1]. \quad (53)$$

Eqs. (50)–(52) are seen to be identical with (25)–(27) of D, provided that in the latter equations, we set $X = y_3'$, $Y = y_2'$, $Z = y_1'$, $\sigma = a$ and $b = 1$.

According to the results of D, the system (50)–(52) possesses stable steady solutions, which we wish to avoid, if $(a - 2)r < a(a + 4)$. In particular, it possesses such solutions for all positive values of r if $a < 2$. On the other hand, (16) cannot be satisfied if $a > 4$. An obvious choice for a is 3, whence $c^2 = \frac{3}{4}$. The steady solutions of (50)–(52) are then all unstable if $r > 21$. Whether or not, as in D, the periodic solutions are also unstable may be investigated through numerical integration.

We shall choose the numerical values of the physical constants to conform with the earth's atmosphere in temperate latitudes, to the extent that this is possible. According to (27) $\tau = 1$ when $t = f^{-1}$, and we shall let $f^{-1} = 10800\text{s} = 3$ h. We shall let $g = 10$ m s^{-2}, $L = 1080$ km, and $H = 8$ km, so that $g_0 = 8$. We shall let $\kappa = \nu = 2.25 \times 10^6$ m^2 s^{-1}, so that $\kappa_0 = \nu_0 = \frac{1}{48}$, implying a 6-day diffusive damping time for y_1 and y_2 and a 2-day damping time for y_3. Noting that h_1 and F_1 must have opposite signs if $r > 0$, we shall let $h_1 = -1$, whence the topography varies between +2 and −2 km. Then $r = 21$ when $F_1 = 0.10785$. Since the critical value for F_1 in the PE model is likely to differ from that in the QG model, and since in any case we do not wish to restrict our attention to the critical value, we shall work with various values of F_1 differing from 0.10785 by not too large a factor.

To advance our numerical solutions from time τ to time $\tau + \Delta\tau$, where $\Delta\tau$ is a prechosen time increment, we shall use a Taylor-series scheme, which consists of evaluating the first n time derivatives of each variable at time τ and then letting

$$s(\tau + \Delta\tau) = \sum_{k=0}^{n} [d^k s(\tau)/d\tau^k]\Delta\tau^k/k!, \quad (54)$$

where s stands for any dependent variable. This scheme is especially convenient for estimating values of s within time steps, such as at zero crossings or

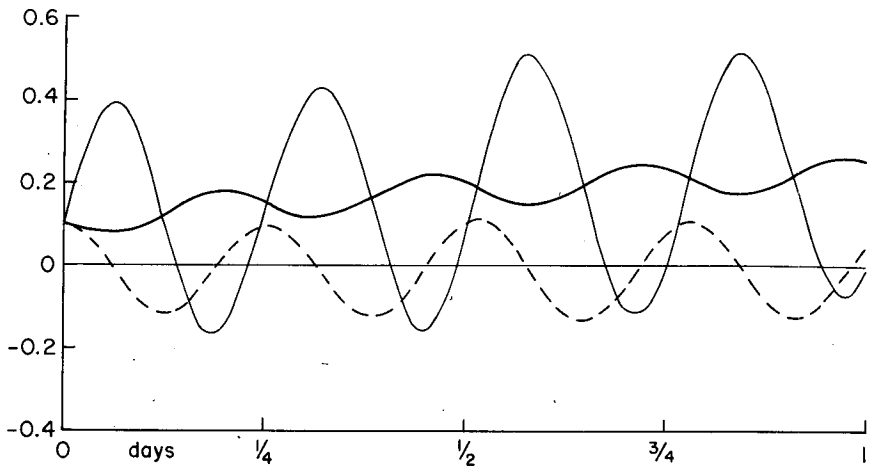

FIG. 1. Variations of x_1 (dashed curve), y_1 (heavy solid curve) and z_1 (thin solid curve) during first day of first numerical solution of PE model.

maxima or minima, since, having in any case evaluated the derivatives, we may simply replace $\Delta\tau$ by an appropriate fraction of $\Delta\tau$ in (54). In all of our solutions we shall let $n = 4$.

For (33)–(35) we shall choose $\Delta\tau = 1/12$ (i.e., 15 min), while for (43) we shall choose $\Delta\tau = 1$ (i.e., 3 h). These values are considerably smaller than those needed for computational stability, but we are interested in more than stability; we wish a rather accurate picture of the attractor.

5. Behavior of the model

For most of our solutions of (33)–(35) we have chosen $F_1 = 0.10$, after discovering that somewhat larger values including 0.11 and 0.125, which might have appeared more likely to lead to aperiodicity, actually produced stable periodic solutions. We found, incidentally, that with $F_1 = 0.40$ the solution went to infinity. This blow-up was not computational; the solution was virtually reproduced when $\Delta\tau$ was lowered to 1/24. In view of our earlier discussion, this behavior was to be expected for sufficiently strong forcing.

For our first numerical integration with $F_1 = 0.10$, we have rather arbitrarily chosen the initial value of each variable to be 0.10, and have run the integration for 400 days (38 400 iterations). Fig. 1 shows the behavior of x_1, y_1, and z_1 for the first day. The variations are dominated by pronounced oscillations with a period close to 6 h. These are plainly ageostrophic, since y_1 and z_1 are opposite in phase, and they are evidently gravity-wave oscillations.

Fig. 2 extends the variations of y_1 and z_1 to eight days. The gravity waves exhibit considerable damping, and we see that they are superposed on longer period variations where y_1 and z_1 are in phase and

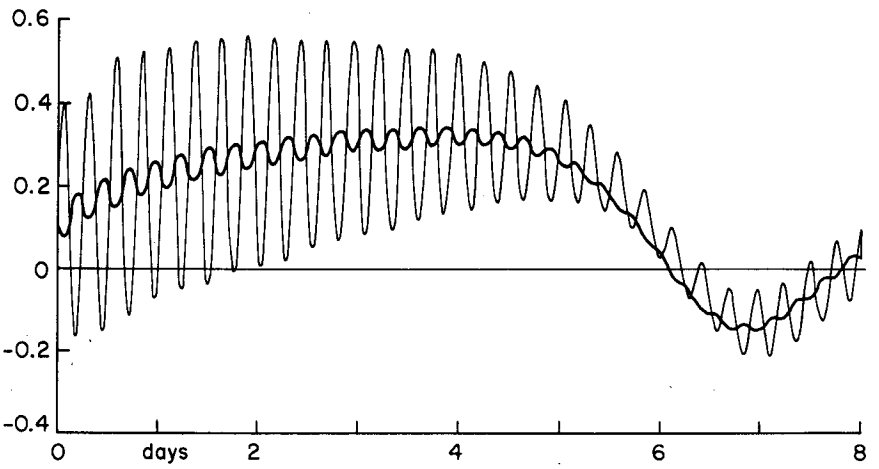

FIG. 2. Variations of y_1 (heavy curve) and z_1 (thin curve) during first eight days of first numerical solution of PE model.

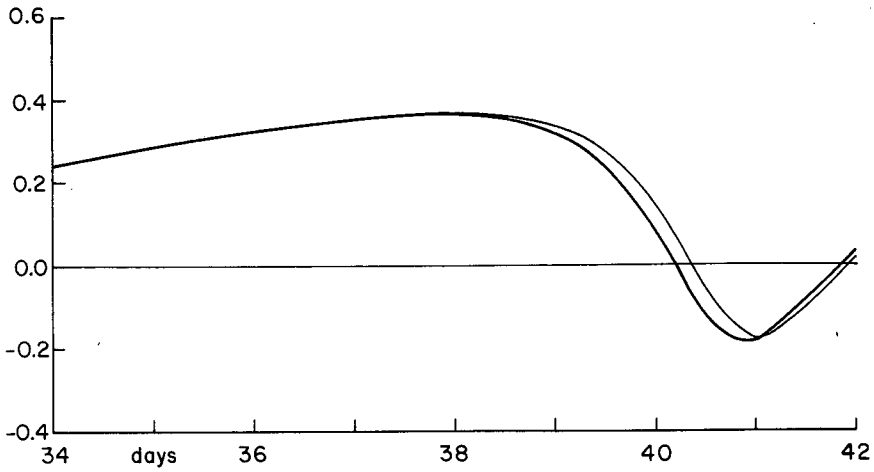

FIG. 3. Variations of y_1 (heavy curve) and z_1 (thin curve) from $t = 34$ days to $t = 42$ days in first numerical solution of PE model. The difference between the curves is unresolvable from 34 to 38 days.

nearly equal, and which therefore are presumably quasi-geostrophic.

Fig. 3 is like Fig. 2 except that the variations of y_1 and z_1 are from day 34 to day 42. The quasi-geostrophic variations are almost like the earlier ones, but the gravity waves seem to have vanished. Actually they are easily detected in the third significant decimal place of the numerical output, and they dominate the second time derivatives, but they become lost in the round-off after several months.

If it is true that the gravity waves die out altogether as $\tau \to \infty$, while the quasi-geostrophic variations remain, the system should ultimately vary with three degrees of freedom instead of nine. That is, there should be a three-dimensional stable invariant manifold—invariant in that a point on it remains on it while traversing an orbit, and stable in that a point close to it approaches it. The attractor should be contained in this manifold.

On the manifold the values of three variables, say the y's, should determine the values of the remaining six. If analytic expressions for the x's and z's in terms of the y's could be discovered and substituted into the equations governing the y's, a three-variable system would result. The attractor of this new system would be the projection of the nine-variable attractor on the y_1-y_2-y_3-subspace.

Attempts to initialize more general primitive-equation models for forecasting are based on the premise that contemporary relations among the variables do exist, at least approximately, i.e., that large-scale gravity waves are of minor importance. Quasi-geostrophic models may be regarded as crude approximations to the reduced systems which would result. In our case, if the QG model is actually a reasonable approximation to the new three-variable system, the attractor set of the PE model, or its projection on the y_1-y_2-y_3 subspace, should have many features in common with the QG attractor, and hence with the attractor discovered in D. We shall attempt to determine whether our conjectures are correct.

Fig. 4 shows the variations of Y_1 and Y_3 for the first 80 days, which include the days shown in Figs. 2 and 3. We have switched from y_i to Y_i, given by (39), because maxima of Z in D correspond to minima of y_1, and hence to maxima of Y_1. The figure is constructed from values at 6 h intervals, except for the first 5 days, when values at 12 h intervals are used. The initial gravity-wave oscillations are thereby not eliminated, but they show up in "aliased" form as oscillations of considerably longer period.

The quasi-geostrophic oscillations of Y_1 exhibit a succession of clearly defined maxima and minima occurring about once a week, but at irregular intervals, with somewhat similar but not identical shapes and varying intensities. They show no sign of damping. The rather flat initial minimum actually results from the superposition of a maximum in the aliased gravity waves on a more typical quasi-geostrophic minimum.

If Y_3 were replaced by its absolute value, its variations would look very much like those of Y_1. The maxima of $|Y_3|$ are in one-to-one correspondence with those of Y_1, and occur a few hours earlier. Moreover, the higher the maximum of Y_1, the higher that of $|Y_3|$. However, Y_3 also undergoes irregular changes of sign; sometimes there are two successive maxima of $|Y_3|$ where Y_3 has the same sign, and sometimes only one. Examination of Fig. 4 and its continuation indicate that sign changes follow the higher maxima of Y_1; the critical maximum is close to 0.06. The general behavior is like that found in D.

A feature of the numerical solutions studied in D

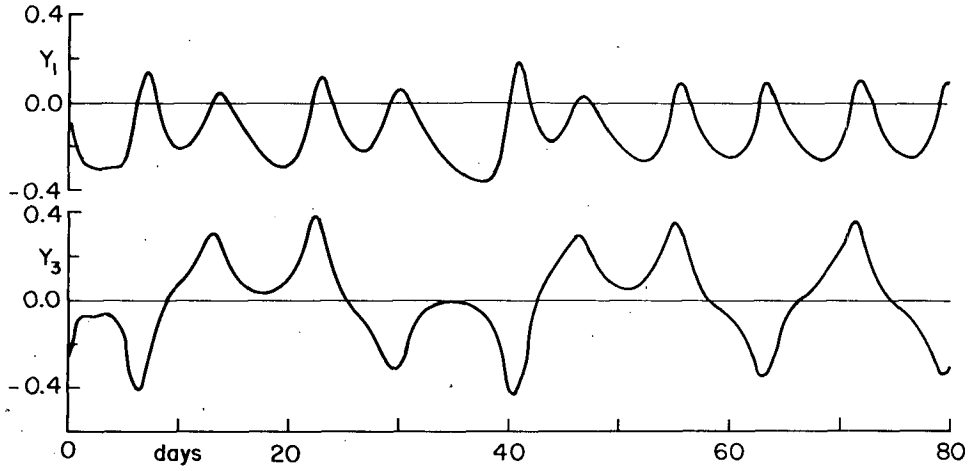

FIG. 4. Variations of Y_1 (upper curve) and Y_3 (lower curve) during first 80 days of first numerical solution of PE model.

is that the value of Z at one maximum is a nearly perfect predictor of the value at the following maximum, i.e., to a close approximation, successive maxima satisfy a first-order difference equation. Once observed, this behavior is not difficult to account for. A point P at which Z acquires a specified maximum value, say Z^*, lies on three surfaces—the plane $Z = Z^*$, the hyperboloid $dZ/dt = 0$, and the attractor. It must therefore be one of the limited number of points in which these surfaces interact. Actually the attractor is an infinite complex of surfaces, but it is closely approximated by a pair of smooth surfaces, one of which may be obtained from the other by rotating through 180° about the Z-axis. The plane, hyperboloid, and approximate attractor prove to intersect in only four points. Two of these, with equal values of Z, are at maxima; the other two are at minima. To within the 180° rotation, then, P is determined by Z^*, and so, therefore, are the properties of the orbit passing through P, including the next maximum value of Z.

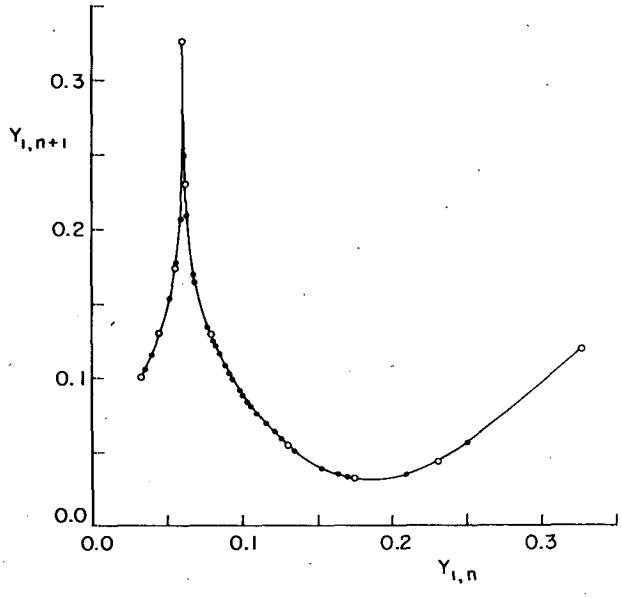

FIG. 5. Pairs of successive maxima of Y_1 in numerical solutions of PE model. Abscissa is nth maximum $Y_{1,n}$; ordinate is following maximum $Y_{1,n+1}$. Pairs from first and second numerical solutions are indicated by closed and open circles, respectively. Smooth curve fitting points is sketched in.

Fig. 5 shows that this feature also characterizes our PE model. It has been constructed as a scatter diagram, but the points reveal no scatter. The solid circles indicate points whose coordinates are two successive maxima of Y_1. Only those maxima occurring after 50 days, when the influence of the gravity waves is invisible, are shown; some points which would have fallen nearly on top of other points are omitted.

The open circles are obtained from a second numerical integration, which was also run for 400 days. The equations possess a steady solution in which the flow is purely zonal and nearly geostrophic; this is given by $x_1 = -0.01111$, $y_1 = 0.53331$, $z_1 = 0.53354$, while each variable with a subscript 2 or 3 vanishes. It corresponds as closely as is possible in the model to the theoretical "Hadley circulation" in an idealized atmosphere.

The corresponding solution in the QG model is $y_1 = 0.53333, y_2 = y_3 = 0$. This corresponds in turn to the violently unstable state of no motion in the convective model in D, where all variables vanish. In the QG and PE models the steady Hadley solutions are likewise unstable. For the second numerical solution we have chosen as an initial state a very small departure from the Hadley solution, by letting $y_2 = z_2 = -0.00001$. The open circles in Fig. 5 show pairs of maxima of y_1 from this solution. A smooth

curve which has been sketched through the open circles fits the solid circles equally well.

As in D, the curve possesses a single cusp. The abscissa, 0.060, is evidently the value of the maximum of Y_1 which separates those maxima of Y_1 where Y_3 subsequently changes sign from those where it does not. Just at the critical value, Y_3 cannot decide whether to change or retain its sign, and so it does neither; instead it approaches zero, and the orbit approaches the intersection of the Y_1-axis and the attractor, i.e., the steady Hadley solution. Maxima close to 0.060 are therefore followed by close encounters with the Hadley solution, and subsequently by behavior resembling the initial days of our second numerical solution. The extreme maximum, 0.326, which is the first maximum attained in the second solution, is therefore shown as following a maximum of 0.060. Incidentally, the Hadley solution is an example of a fixed point which, although unstable, lies on the attractor.

We have noted that the general solution can be aperiodic only if all periodic solutions are unstable. In a periodic solution the succession of maxima of Y_1 is also periodic, and therefore determines a finite set of points $P_1, \ldots, P_N$ on the curve in Fig. 5. If the initial state is perturbed slightly, so that the abscissa of one point P_k is displaced by an amount ϵ, the abscissa of P_{k+1}, which is the ordinate of P_k, will be displaced by the product of ϵ and the slope λ_k of the curve at P_k. It follows that a periodic solution is unstable if the product $\lambda_1, \ldots, \lambda_N$ exceeds unity in absolute value.

The curve in D proved to have a slope exceeding unity everywhere, so there was no question about the product. A feature of the curve in Fig. 5 not found in D is the singularity, i.e., the point where the slope vanishes. This introduces the possibility of stable periodic solutions, since large slopes near the cusp may be cancelled by small slopes near the singularity. In particular, if one point of a periodic solution coincides with the singularity, the product of the slopes will vanish, unless another point coincides with the cusp.

It is not likely that for a given choice of F_1 the singularity will coincide with a point on a periodic solution, since the number of such points should be countable. However, if the Nth point following the singularity lies close to the singularity, a properly chosen small change in F_1 should suffice to move the Nth point to the singularity, thereby producing a stable periodic solution. We have discussed this question in detail in a study of a quadratic difference equation (Lorenz, 1964).

Since we do not know what values of F_1 near 0.10 will produce stable periodic solutions with very long periods, we cannot be certain that 0.10 is not one of these values, and that the apparent aperiodicity in our numerical solutions is more than a transient phenomenon. We can be fairly sure that for some values of F_1 very close to 0.10 there are no stable periodic solutions. The long-term behavior for these values of F_1 will be virtually indistinguishable from the transient behavior for the values of F_1 producing stable periodic solutions. We can be fairly sure, then, that our numerical solutions represent long term behavior, with the possible provision that it is the behavior for some value of F_1 like 0.10002 rather than 0.10.

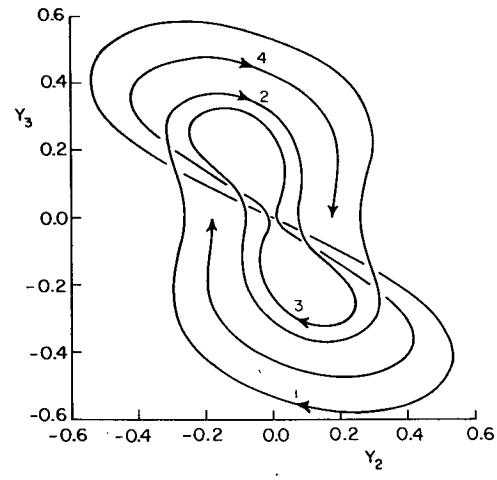

FIG. 6. Projection on Y_2-Y_3 plane of two orbits emanating from unstable fixed point representing Hadley solution, for PE model with $F_1 = 0.10$. Where two curves cross, curve with lower value of Y_1 is broken. The origin of the orbits is at center of symmetry of figure. Arrowheads labeled 1, 2, 3, 4 indicate locations of first through fourth maxima of Y_1 on orbit where Y_2 is initially positive.

6. The attractor set

Since we cannot easily make nine-dimensional drawings, we shall examine the projections of orbits, and of the attractor, on various three-dimensional subspaces. Let us regard Y_2 and Y_3 as horizontal coordinates and Y_1 as the vertical coordinate in the Y_1-Y_2-Y_3-subspace. Fig. 6 shows the horizontal projection of a portion of the orbit in the second numerical solution, and of another orbit differing from this one only in the signs of Y_2 and Y_3. Where two curves cross, the lower one has been broken. The numbered arrowheads show the locations of the first four maxima of Y_1 in the first solution.

Fig. 7 shows the projection of the attractor on the Y_1-Y_2-Y_3 subspace. A portion with positive values of Y_3 is omitted, since the attractor is unchanged by a 180° rotation about the origin. The drawing requires some explanation.

As in D, the attractor is actually an infinite complex of surfaces, but, for any choice of Y_2 and Y_3, each possible value of Y_1 is very close to a single value, or to one of two values. In the region where only one such value exists, the thin solid lines are

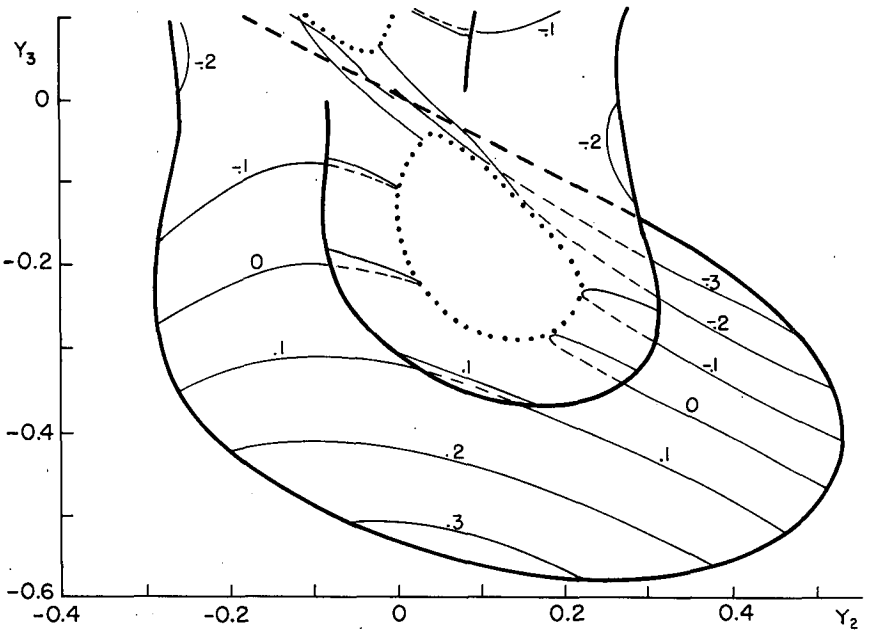

FIG. 7. Projection of PE model attractor on Y_1-Y_2-Y_3 subspace, for $F_1 = 0.10$. Coordinates are Y_2 and Y_3. Thin solid curves are contours of Y_1, or, where two surfaces exist, contours of Y_1 on upper surface. Thin dashed curves are contours of Y_1 on lower surface. Heavy dashed curve and extensions as heavy solid curves are natural boundaries of attractor. Heavy dotted curve is boundary of projection of attractor on Y_2-Y_3 plane. Portion of figure with $Y_3 > 0.10$ is omitted, since it may be obtained by rotating figure through 180° about origin. See text for details.

contours of Y_1; where two values exist, they are contours of the higher value of Y_1, while thin dashed lines are contours of the lower value.

If any initial state very close to the steady Hadley solution is chosen, the orbit proceeding from it will for a while be almost identical with one of the orbits in Fig. 6. The heavy dashed curves emanating from the origin, and their extensions as heavy solid curves, are the initial portions of these orbits. Since the first maxima of $|Y_2|$ and $|Y_3|$ on these orbits are the extreme maxima, the heavy solid curves form natural boundaries for the attractor. The extensions of the heavy solid curves into the interior of the figure form natural boundaries for the upper surface. The curves have been terminated where the upper and lower surfaces for practical purposes merge.

The heavy dotted curves indicate where the attractor is vertical, i.e., they are natural boundaries for the projection of the attractor on the Y_2-Y_3 plane. They are not projections of single orbits, but are envelopes of such projections. No orbits enter the holes which they enclose.

Let us choose a point on the boundary in the lower portion of Fig. 7, say $Y_2 = 0.10$, $Y_3 = -0.56$, $Y_1 = 0.33$, and move along the attractor toward higher values of Y_3, keeping Y_2 constant. We first move downward, crossing the 0.3 and 0.2 contours of Y_1, and the (dashed) 0.1 contour shortly after sliding under the boundary of the upper surface. We continue downward less steeply, and eventually move horizontally, then upward, and then vertically upward as we reach the dotted curve. To remain on the attractor we must enter the upper surface proceeding back toward lower values of Y_3, and we reach the boundary of this surface just after crossing the (solid) 0.1 contour.

Where the heavy solid curves have been terminated, at $Y_2 = \pm 0.08$, $Y_3 = 0.0$, the upper and lower surfaces of course do not really merge; they simply become too close to be easily resolved. If we follow an orbit past one of these points along what now looks like one surface, until it passes over or under another apparent surface, a pair of surfaces is really passing over or under another pair. These four surfaces subsequently appear to merge, and then pass over or under another set of four surfaces, etc. The surfaces on which an orbit emanating from the origin eventually finds itself thus constitute a countable set, which is analogous to the set of all numbers between 0 and 1 having *terminating* decimal expansions which contain only 0's and 1's. The attractor set is the topological closure of this set of surfaces, and contains all surfaces which are limits of sequences of surfaces in the countable set; it is thus

analogous to the set of numbers with terminating or nonterminating decimal expansions containing only 0's and 1's, and hence is a Cantor set.

Our picture of the attractor is somewhat difficult to compare with the picture in *D*, since there we chose *Y* and *Z*, corresponding to Y_2 and Y_1, as horizontal coordinates. Had we done so in the present case, showing contours of Y_3, we would have found it necessary to show four surfaces instead of two in portions of the figure. The prominent holes bounded by the dotted curves would have penetrated two of these surfaces but not the other two. The resulting picture would have been quite confusing.

We now turn to the remaining variables. Fig. 8 is like Fig. 7, except that it shows contours of Z_3 (we define Z_i as $-a_iz_i$). We find that where a single surface is present in Fig. 7, there is a single value of Z_3; where two surfaces are present there are at most two values of Z_3—one on each surface. We conclude that, to the extent that we can judge from the numerical output, the values of the *Y*'s completely determine Z_3.

If the motion were exactly geostrophic, the contours of Z_3 in Fig. 8 would coincide with lines of constant Y_3. We observe that over much of the figure they come close to doing this; note, for example, the solid -0.3 contour. There are some regions, however, where the motion is less geostrophic; note the dashed -0.3 contour, and the nearby portion of the -0.4 contour. Further examination indicates that those points where Z_3 and Y_3 differ appreciably are located fairly close to the natural boundary of lower surface. Orbits passing through these points, such as the curve passing through $(Y_2, Y_3) = (0.4, -0.3)$ in Fig. 6, tend to remain close to the natural boundary, so that Y_1 should surpass 0.2 or perhaps 0.25 at its next maximum. Comparison with Fig. 5 shows that this can happen only if the previous maximum lies in an extremely narrow range—perhaps between 0.059 and 0.061. Since maxima of Y_1 in a much wider range containing 0.60 are more or less equally probable, we conclude that a maximum exceeding 0.25, and hence a strongly ageostrophic value of Z_3, is a rather rare event.

It is of interest at this point to compare the geostrophic equation and the balance equation. The latter may be obtained from (33) by discarding all terms containing the *x*'s, but retaining the nonlinear terms not containing the *x*'s. The resulting equation is

$$a_iy_i - 2c^2y_jy_k = a_iz_i, \tag{55}$$

where again (i,j,k) is any cyclic permutation of (1,2,3). It is easily solved for the *y*'s in terms of the *z*'s for those values of the *z*'s for which solutions exist. These include all values encountered in our second numerical solution. We shall let z_i' denote the value of y_i satisfying (55); the value satisfying the geostrophic equation is of course z_i.

It was our intention to present a figure like Fig. 8 showing the contours of Z_3' $(= -a_3z_3')$ instead of Z_3. We found, however, that the contours were hardly distinguishable from the lines of constant Y_3, and that there were no interesting details to demonstrate. We conclude that the balance equation is a

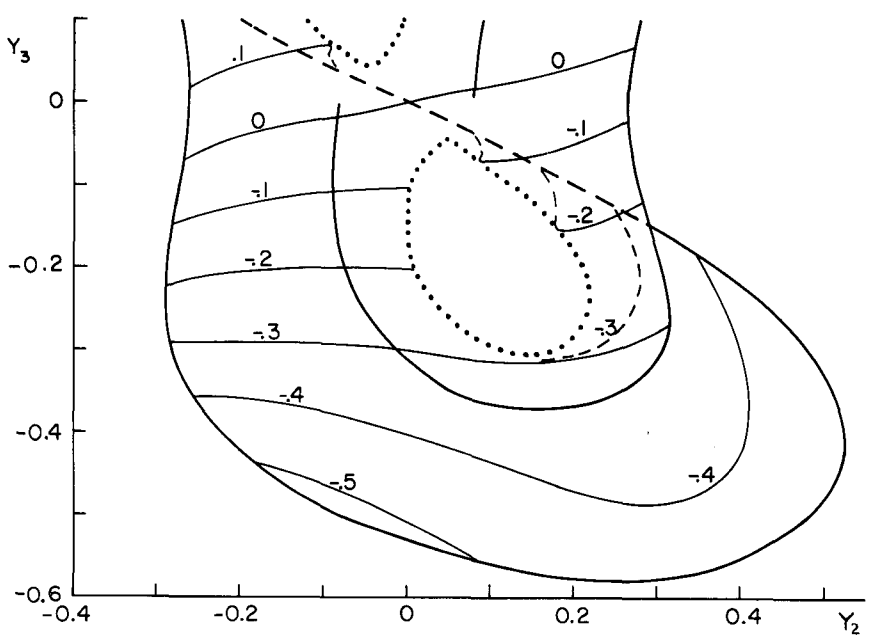

FIG. 8. As in Fig. 7, but with contours of Z_3.

good approximation everywhere on the attractor. The strongly ageostrophic states result from nonlinearity, which manifests itself in one term of the balance equation.

Fig. 9 shows contours of Z_2. For geostrophic conditions these should coincide with lines of constant Y_2, and we see that they fit these lines reasonably well. Like Z_3, the value of Z_2 is completely determined by the Y's.

Similar remarks apply to Z_1 and the X's. The latter variables would vanish under purely geostrophic conditions, and actually they are small compared to the Y's.

We conclude first that on the attractor the values of the y's completely determine the values of the remaining six variables. In addition, the nine variables are in approximate geostrophic equilibrium at most points of the attractor, i.e., the attractor is quasi-geostrophic.

It remains to be seen whether the attractor of the PE model resembles that of the QG model. For identical values of the parameters it evidently does not, since in the latter model the forcing $F_1 = 0.10$ is subcritical. The two steady-state solutions with eddies are stable, and the attractor consists of just these two points.

We shall attempt to find a value of F_1 for the QG model which makes the attractor as much as possible like the PE attractor when $F_1 = 0.10$, in a qualitative sense. We shall do this by finding a value of F_1 which makes the curve of successive maxima of Y_1 look like Fig. 5.

Fig. 10 shows these curves for $F_1 = 0.10, 0.15$ and 0.20. Although more suitable numerical values of Y_1 occur for the lower values of F_1, a more appropriate shape occurs when $F_1 = 0.20$.

Fig. 11 is constructed like Fig. 7, and it shows the QG model attractor, for $F_1 = 0.20$. Although the pictures are not so much alike that one would be mistaken for the other, the qualitative resemblance is evident. The natural boundaries formed by the orbits emanating from the origin possess the same general shape, and each attractor has two prominent holes.

It is likely, then, that the collection of attractor sets which occurs over a considerable range of F_1 in the QG model is rather like a similar collection for the PE model. Similar shapes occur, and there are critical values of F_1 separating one shape from another. The critical values are not the same in the two models, and evidently may differ by a factor of about 2. We found, for example, that the PE attractor reduces to two fixed points for $F_1 < 0.056$. If a single value of F_1 is selected, then, the attractors of the two models may differ considerably.

7. The invariant manifold

Although we know that the attractor is invariant, and have found that the values of three variables on the attractor determine the values of the remaining six, we have not thereby demonstrated that the attractor is embedded in an invariant three-dimensional manifold. We can do this by showing that even for points not on the attractor, if gravity waves are completely absent, the values of three variables

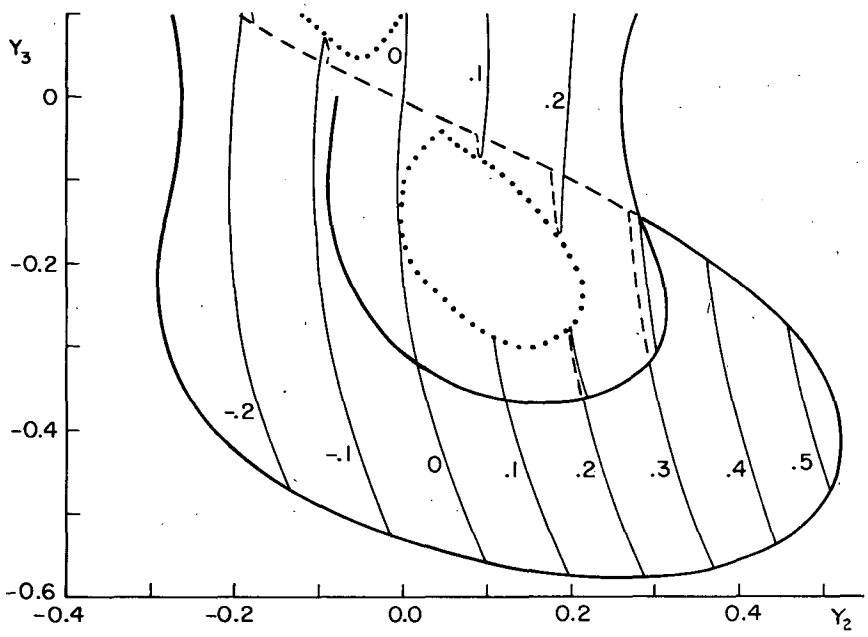

FIG. 9. As in Fig. 7, but with contours of Z_2.

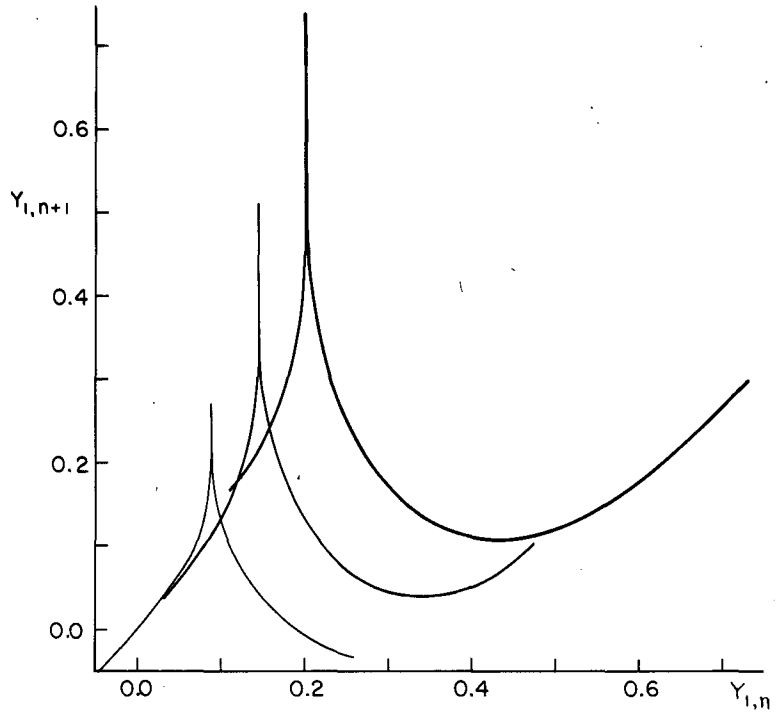

FIG. 10. Curves fitting pairs of successive maxima of Y_1 in numerical solutions of QG model, for $F_1 = 0.10$ (thin curve), $F_1 = 0.15$ (medium curve), and $F_1 = 0.20$ (heavy curve). Abscissa is nth maximum $Y_{1,n}$; ordinate is following maximum $Y_{1,n+1}$.

determine the other six uniquely. Establishing a method to find these values would amount to solving the initialization problem for our PE model.

Gravity waves and quasi-geostrophic oscillations in this model are distinguished by their frequencies, which differ by about an order of magnitude. It follows that, in a particular solution, if the value of one variable, say x_1, can be resolved into gravity-wave and quasi-geostrophic components, the ratio of these components will be exceeded by about n orders of magnitude by the ratio of the same components of $d^n x_1/d\tau^n$. Hence, relative to its value in an arbitrary solution, the value of $d^n x_1/d\tau^n$ in a solution without gravity waves should be close to zero for large n. This property leads to an algorithm for finding points on the manifold.

We choose fixed values of y_1, y_2, y_3, and seek the remaining variables. For notational convenience we let $z_i - y_i = x_{i+3}$ for $i = 1, 2, 3$, and let $\mathbf{Y}$ and $\mathbf{X}$ be three- and six-dimensional vectors with components

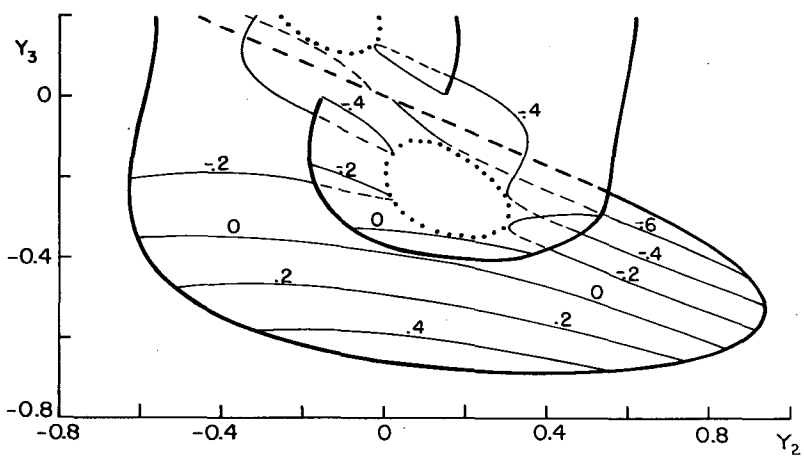

FIG. 11. As in Fig. 7, but for QG model with $F_1 = 0.20$.

(y_1,y_2,y_3) and $(x_1, \ldots, x_6)$. For a starting approximation we choose $\mathbf{X} = 0$, and in successive approximations we determine $\mathbf{X}$ so that $d\mathbf{X}/d\tau = 0$, $d^2\mathbf{X}/d\tau^2 = 0$, etc.

To find these values of $\mathbf{X}$ numerically we use a double approximation procedure. We let $X_{n,k}$ be the kth approximation to the value of $\mathbf{X}$ which makes $d^n\mathbf{X}/d\tau^n$ vanish. We set $\mathbf{X}_{1,0} = 0$, i.e., we begin with the geostrophic approximation, and in general we let

$$\mathbf{X}_{n,k+1} = \mathbf{X}_{n,k} - (d^n\mathbf{X}_{n,k}/d\tau^n)[\partial(d^n\mathbf{X}_{n,k}/d\tau^n)/\partial\mathbf{X}_{n,k}]^{-1},$$

where the quantity in brackets is a sixth-order square matrix, which may be estimated by perturbing the components of $\mathbf{X}$ one at a time, and reevaluating the components of $d^n\mathbf{X}/d\tau^n$. When the procedure has converged for a particular value of n, say, when $k = K(n)$, we let

$$\mathbf{X}_{n+1,0} = \mathbf{X}_{n,K(n)} \tag{57}$$

and continue.

We have applied our algorithm to a number of values of $\mathbf{Y}$, some of which lie on the projection of the attractor on the y_1-y_2-y_3 subspace, and some of which do not. In general the procedure converges rapidly; three or four values of k are sufficient for each value of n, and the computed components of $\mathbf{X}$ do not vary appreciably after $n = 3$. When $\mathbf{Y}$ is on the attractor, the components of $\mathbf{X}$ yielded by the algorithm agree to five decimal places with those appearing in numerical solutions where the orbit has reached the attractor.

When $\mathbf{Y}$ is not on the attractor, we have used the components of $\mathbf{Y}$, together with the components of $\mathbf{X}$ yielded by the algorithm, as initial conditions in a new numerical integration. After a number of days, but before the attractor has been reached, we have stopped the integration. We have then applied the algorithm to the final values of $\mathbf{Y}$. The components of $\mathbf{X}$ which it yields have again been identical with the final components of $\mathbf{X}$ in the numerical integration. The invariance of the manifold is thus confirmed.

Numerous variations of the algorithm are possible. We have tested one in which the quantities which are made to vanish in the nth approximation are $d^{n-1}x_i/d\tau^{n-1}$ and $d^nx_i/d\tau^n$, for $i = 1, 2, 3$. Applied to the same values of y_1, y_2, y_3, it yields the same results as the first algorithm.

We shall call the equation which describes the invariant manifold the *superbalance* equation. Although we have not managed to write it in explicit form, we know that it looks somewhat like the geostrophic equation. It should look more like the balance equation; in introducing the balance equation, Charney (1955) found that if in a simple system it was initially satisfied, it would continue for some time to be nearly satisfied, so that it would describe a nearly invariant manifold. The superbalance equation is not the balance equation, however, since the latter is completely fixed by the divergence equation (33), while the former would be altered by any change in the system (33)–(35), including the intensity of the forcing.

As to the stability of the invariant manifold, it appears that if an initial state close to the manifold is chosen, the orbit may temporarily move toward or away from the manifold, but in due time it will approach the attractor, and so will necessarily approach the manifold, which contains the attractor. We conclude that there exists a stable invariant three-dimensional manifold composed of all states from which gravity-wave oscillations are completely lacking. Embedded in this manifold is the attractor set, which consists of an infinite complex of two-dimensional surfaces, but is closely approximated by a pair of surfaces.

8. Concluding remarks

The attractor set of a dynamical system is for practical purposes the set of points in phase space which will continue to be encountered by an arbitrary orbit after an arbitrarily long time has passed. For a large class of forced dissipative systems the attractor has zero volume, i.e., an arbitrarily selected point in phase space is almost always not on the attractor. When the general solution is aperiodic, the attractor is strange.

The dynamical system which we have chosen to investigate is one of the simplest possible nonlinear primitive-equation models. It possesses nine dependent variables. We have found, as expected, that the attractor is confined to a central region of phase space, and that most of its points represent states of approximate geostrophic equilibrium. Where the geostrophic relation fails, the balance equation is a good approximation.

We have also found that the system possesses a three-dimensional stable invariant manifold, representing states which are devoid of gravity waves. The attractor is embedded in this manifold. Points on the manifold, whether or not they are on the attractor, tend to satisfy the geostrophic equation; again, the balance equation is more closely satisfied.

We have constructed a three-variable quasi-geostrophic model by replacing the prognostic divergence equation by the geostrophic equation. The attractor of this model is qualitatively like that of the PE model, provided that the intensity of the forcing is suitably adjusted. It appears that a three-variable model in which the divergence equation is replaced by the balance equation would possess an attractor more nearly resembling the PE attractor, although we have not pursued this question. The

perfect three-variable model would of course be the one where the superbalance equation is used; there the attractors of the three- and nine-variable models would be identical.

The question naturally arises as to what the attractor of a more realistic meteorological model, perhaps a global circulation model (GCM) with 100 000 variables, would look like. We feel certain that for appropriate choices of the constants the model would vary aperiodically, and the attractor would be strange. The model should admit many modes of motion which decay with time, so that the attractor should have few dimensions compared to the entire space. Perhaps it would have several hundred dimensions. Topologically it might be the product of a few hundred continua and a number of Cantor sets.

We know of no useful way to draw a picture of the projection of the attractor on a subspace of several hundred dimensions. If we project the attractor onto a plane, or onto any subspace with fewer dimensions than the attractor itself, the projection will fill a continuous region in the subspace, and the strangeness, i.e., the presence of Cantor sets, will not be detectable.

The phase space of the GCM should also contain an invariant manifold, representing states which are devoid of gravity waves. The stability of this manifold is another matter. Gravity waves are present to some extent in the real atmosphere, and they should appear in a realistic GCM. If the manifold is unstable, the attractor will not be embedded in it.

The simple algorithm which we used to find the invariant manifold presumably does not solve the initialization problem for larger models such as the GCM's. It is based on the complete separation of quasi-geostrophic and gravity-wave frequencies. A GCM will admit internal gravity waves, with lower frequencies. Small-scale weather features will, simply by being advected, oscillate more rapidly than large-scale features. The gravity-wave and weather-system frequencies are therefore likely to overlap. It would still be interesting to see what this initialization procedure would produce.

For models which are much simpler than a GCM, but more detailed and presumably more realistic than our nine-variable model, the problem of drawing a picture of the attractor seems more tractable. Perhaps the next task to be accomplished is the discovery and description of an attractor which is topologically the product of more than two continua, and, if possible, more than one Cantor set.

Acknowledgment. This research has been sponsored by the Climate Dynamics Program of the National Science Foundation under Grant NSF-g 77 10093 ATM.

REFERENCES

Charney, J. G., 1955: The use of the primitive equations of motion in numerical weather prediction. *Tellus*, **7**, 22–26.

——, and J. G. Devore, 1979: Multiple flow equilibria in the atmosphere and blocking. *J. Atmos. Sci.*, **36**, 1205–1216.

Lorenz, E. N., 1960: Maximum simplification of the dynamic equations. *Tellus*, **12**, 243–254.

——, 1963: Deterministic nonperiodic flow. *J. Atmos. Sci.*, **20**, 130–141.

——, 1964: The problem of deducing the climate from the governing equations. *Tellus*, **16**, 1–11.

Vickroy, J. G., and J. A. Dutton, 1979: Bifurcation and catastrophe in a simple, forced, dissipative quasi-geostrophic flow. *J. Atmos. Sci.*, **36**, 42–52.

von Arx, W. F., 1952: A laboratory study of the wind-driven ocean circulation. *Tellus*, **4**, 311–318.